AIChE

Cubic-Plus-Association Equation of State for Water-Containing Mixtures: Is ‘‘Cross Association’’ Necessary?

Zhidong Li and Abbas Firoozabadi
Reservoir Engineering Research Institute (RERI), Palo Alto, CA 94306

DOI 10.1002/aic.11784

We have recently proposed an accurate version of the cubic-plus-association (CPA) equation of state (EOS) for water-containing mixtures which combines the Peng-Robinson equation (PR) for the physical interactions and the thermodynamic perturbation theory for the hydrogen bonding of water molecules. Despite the significant improvement, the water composition in the nonaqueous phase is systematically underestimated for some systems where the nonwater species are methane and ethane at very high pressures, unsaturated hydrocarbons, CO_2, and H_2S. We attribute the deficiency to the neglect of the ‘‘cross association’’ between water and those nonwater molecules. In this work, the accuracy is drastically improved by treating methane, ethane, unsaturated hydrocarbons, CO_2 and H_2S as ‘‘pseudo-associating’’ components and describing the cross association with water in the framework of the perturbation theory. It is shown that the cross association is more significant for the nonaqueous phase. In addition to binary mixtures, reliable predictions are achieved for $H_2O/C_1/CO_2/H_2S$ quaternary mixture in two and three phases.
AIChE J, 55: 1803–1813, 2009
Keywords: petroleum, phase equilibrium, aqueous solutions

Introduction

The importance of water-containing mixtures is widely recognized in many disciplines particularly in the fields of energy and environment. However, it has been challenging to accurately describe the phase behavior of such systems by using theoretical approaches due to complicated nonidealities from the strong hydrogen bonding of water molecules. The cubic-plus-association (CPA) equation of state (EOS) is a powerful tool compared with alternatives[1]; the existing versions demonstrate only limited success due to the poor performance for some cases [Li ZD and Firoozabadi A (2008); Sun LX and Firoozabadi A (2006)].[2–6]

In a recent work, we have proposed an accurate version of CPA for water-containing mixtures in which the physical contribution and the hydrogen bonding of water molecules are described by the Peng-Robinson equation (PR) and the thermodynamic perturbation theory (TPT), respectively. By introducing the higher order temperature-dependent corrections to estimate the energy parameter of pure water in the physical part, the accuracy is drastically improved. The improvement is demonstrated by comparing the calculations and experiments for various binary, ternary and quaternary water/saturated-hydrocarbon mixtures in two and three phases under a wide range of temperatures and pressures.[7]

Despite the significant improvement, the composition of water in the nonaqueous phase is systematically underestimated for nonwater species including methane and ethane at very high pressures, unsaturated hydrocarbons, CO_2, and

---

Additional Supporting Information may be found in the online version of this article.

A. Firoozabadi is also affiliated with Dept. of Chemical Engineering, Yale University, New Haven, CT 06520.

Correspondence concerning this article should be addressed to A. Firoozabadi at abbas.firoozabadi@yale.edu

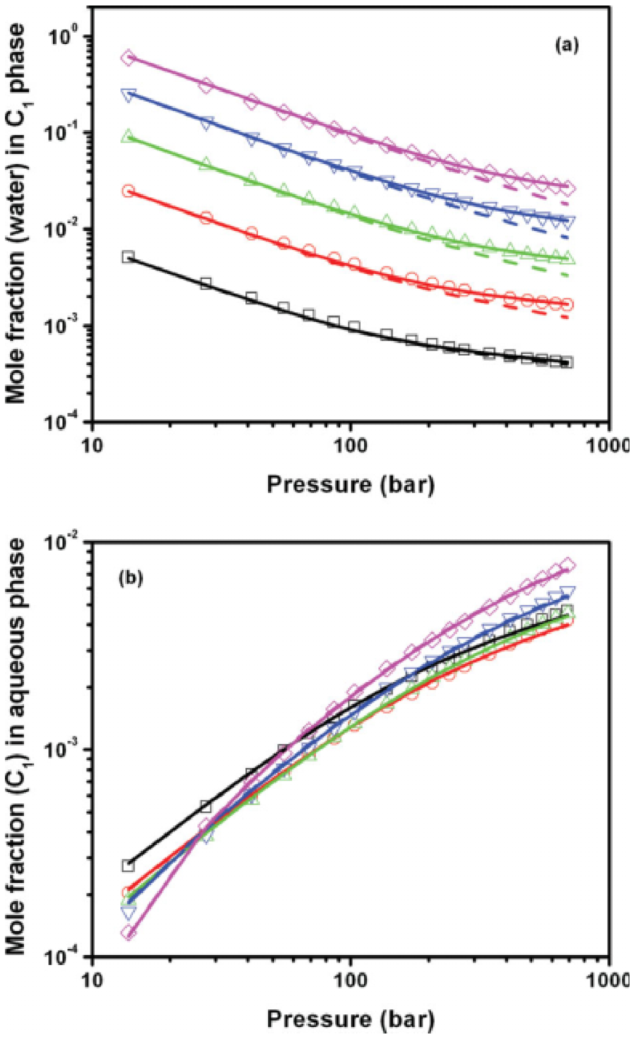

Figure 1. Compositions of (a) C_1 phase and (b) aqueous phase of H_2O/C_1 mixture.

C_1 phase is vapor. Symbols represent experiments from Refs. 19, 20. Solid and dashed lines represent calculations with and without cross association, respectively. Symbols □, ○, △, ▽ and ◇ along with corresponding lines are for 310.93, 344.26, 377.59, 410.93, and 444.26 K, respectively. [Color figure can be viewed in the online issue, which is available at www.interscience.wiley.com.]

H_2S. The deviation from the experiments becomes very large especially for mixtures containing aromatic hydrocarbons, CO_2 and H_2S in the liquid–liquid phase region. We ascribe this deficiency to the neglect of an explicit cross association with water beyond the physical interactions. The origin of the cross association can be either from the water-induced temporary polar moments of hydrocarbon molecules or from the permanent polar moments of CO_2 and H_2S molecules. For the nonwater species examined, we suspect that H_2S has the strongest cross association energy with water, followed by aromatic hydrocarbons and CO_2, and then alkenes. For saturated hydrocarbon components, the cross association with water could be negligible except for methane and ethane at very high pressures.[7]

In this work, we improve our original CPA approach by applying the "pseudo-association" concept to explicitly consider the cross association between water and nonwater species.[8–12] The remainder of this article is organized as the following. We first introduce the molecular modeling and the basic formalism of the theory for the pseudo-association. Next, the performance is illustrated by comparison with the experiments for the phase compositions of H_2O/C_1, H_2O/C_2, H_2O/CO_2, H_2O/H_2S, H_2O/1-hexene, H_2O/1-octene, H_2O/1-decene, H_2O/benzene, H_2O/ethylbenzene, H_2O/*m*-diethylbenzene, H_2O/1-methylnaphthalene, H_2O/1-ethylnaphthalene, and $H_2O/C_1/CO_2/H_2S$ mixtures in two and three phases. Based on accurate description of the phase behavior, the density change when water is saturated with CO_2 is also investigated. The work is concluded with some remarks.

Molecular Modeling and Theoretical Background

We consider the mixtures with nonwater species such as linear 1-alkenes, aromatic hydrocarbons, methane, ethane,

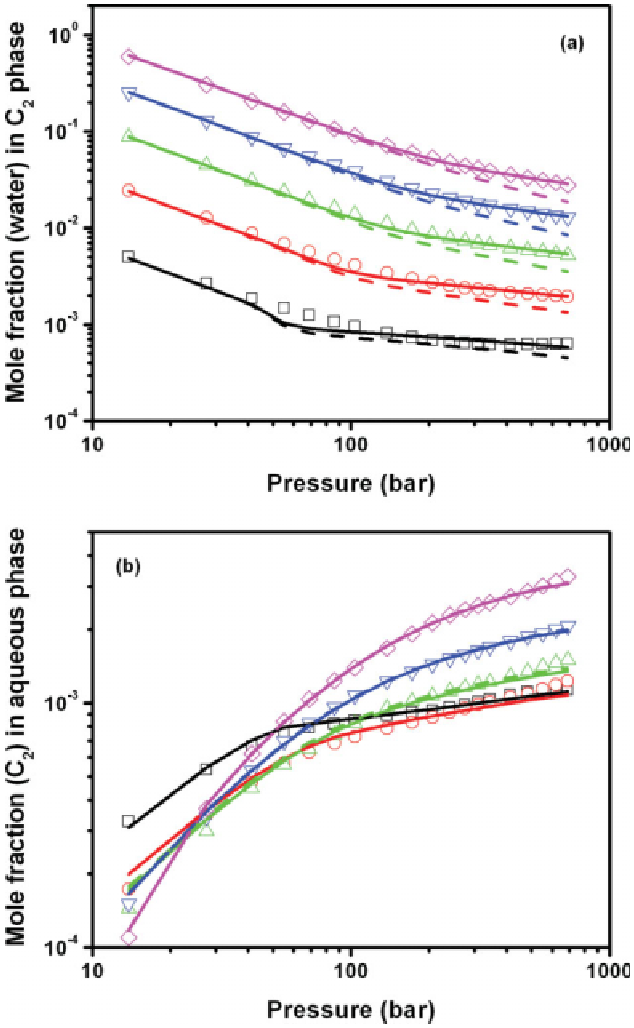

Figure 2. Same as Figure 1 but for H_2O/C_2 mixture.

C_2 phase can be either vapor or liquid. Experiments are from Refs. 21, 22. [Color figure can be viewed in the online issue, which is available at www.interscience.wiley.com.]

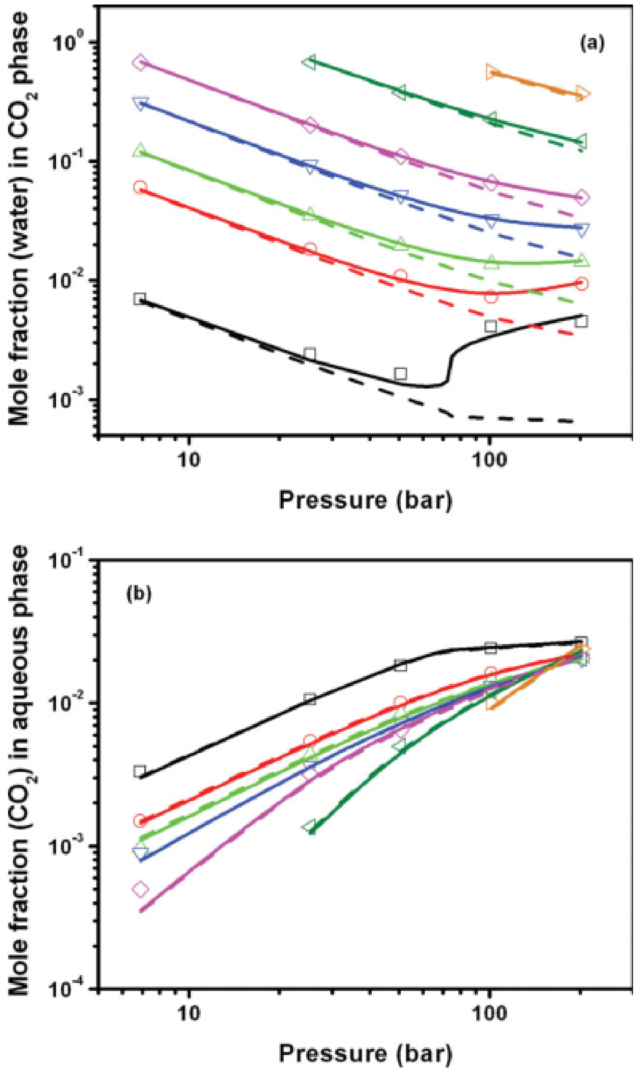

Figure 3. Same as Figure 1 but for H_2O/CO_2 mixture.

CO_2 phase can be either vapor or liquid. Experiments are from Ref. 23. Symbols □, ○, △, ▽, ◇, ◁ and ▷ along with corresponding lines are for 304.21, 348.15, 366.48, 394.26, 422.04, 477.59 and 533.15 K, respectively. [Color figure can be viewed in the online issue, which is available at www.interscience.wiley.com.]

CO_2, or H_2S or any combination and treat these substances as pseudo-associating components. Similar to water molecules, each pseudo-associating molecule is assumed to possess four association sites belonging to two types (α'_i and β'_i) with two sites for each type. As a result, the excess Helmholtz free energy due to association is given by[13–18]

$$\frac{F^{\mathrm{ex}}_{\mathrm{ass}}}{nRT} = 2x_{\mathrm{w}}\left(\ln\chi_\alpha + \ln\chi_\beta - \frac{\chi_\alpha + \chi_\beta}{2} + 1\right) + \sum_i 2x_{\mathrm{ci}}\left(\ln\chi_{\alpha'_i} + \ln\chi_{\beta'_i} - \frac{\chi_{\alpha'_i} + \chi_{\beta'_i}}{2} + 1\right) \quad (1)$$

where n is the total number of moles, R is the universal gas constant, and T is the absolute temperature. x_{w} and x_{ci} represent the mole fractions of water and pseudo-associating component i, respectively. χ_α (χ_β) is the mole fraction of water not bonded at site “α” (“β”) and $\chi_{\alpha'_i}$ ($\chi_{\beta'_i}$) is the mole fraction of pseudo-associating component i not bonded at site “α'_i” (“β'_i”).

We also make two other assumptions. First, there is neither cross association nor self association between pseudo-associating components, i.e., the “association strength” $\Delta^{\alpha'_i\beta'_j} = 0$. Second, the cross association is assumed to be symmetric between two sites of different types of water and pseudo-associating component i, i.e., $\Delta^{\alpha\beta'_i} = \Delta^{\alpha'_i\beta}$. For the symmetric four-site association model for both the water and the pseudo-associating molecules, the nonbonded mole fractions can be calculated from the simplified expressions of the perturbation theory

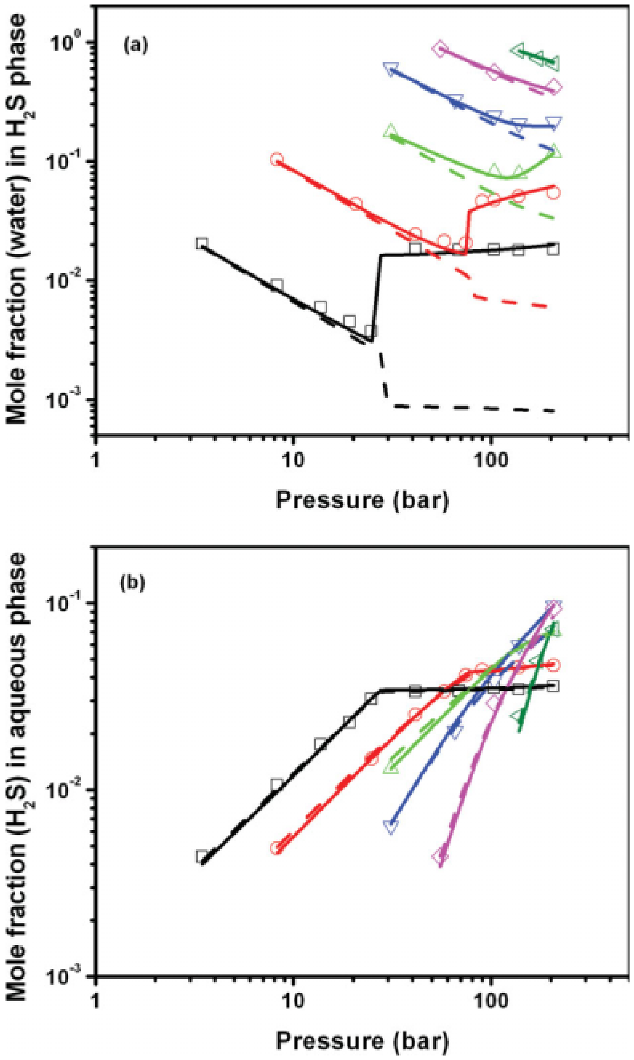

Figure 4. Same as Figure 1 but for H_2O/H_2S mixture.

H_2S phase can be either vapor or liquid. Experiments are from Ref. 23. Symbols □, ○, △, ▽, ◇ and ◁ along with corresponding lines are for 310.93, 366.48, 422.04, 477.59, 533.15 and 588.71K, respectively. [Color figure can be viewed in the online issue, which is available at www.interscience.wiley.com.]

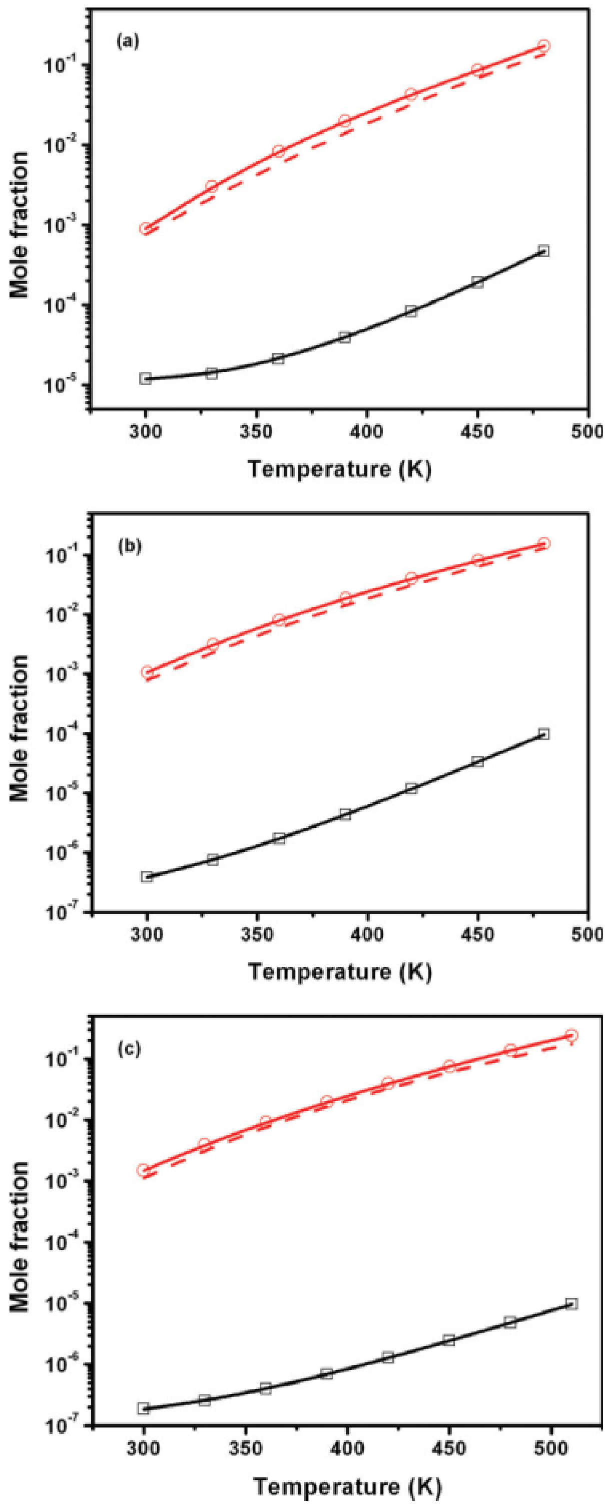

Figure 5. Mutual solubilities for (a) H_2O/1-hexene, (b) H_2O/1-octene, and (c) H_2O/1-decene.

Symbols represent experiments or calibrations from Ref. 24. Solid and dashed lines represent calculations with and without cross association, respectively. Symbols □ and ○ along with corresponding lines are the solubilities of hydrocarbon in water and of water in hydrocarbon, respectively. [Color figure can be viewed in the online issue, which is available at www.interscience.wiley.com.]

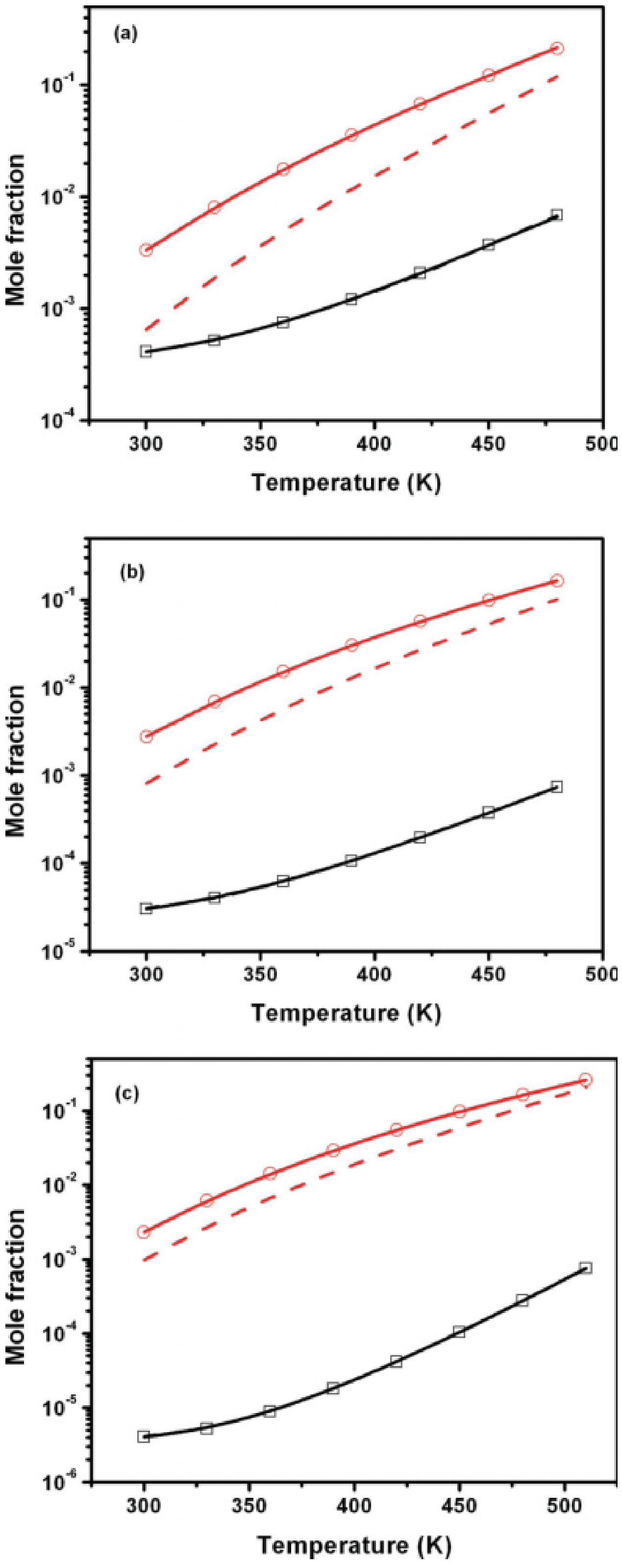

Figure 6. Same as Figure 5 but for (a) H_2O/Benzene, (b) H_2O/Ethylbenzene, and (c) H_2O/*m*-diethylbenzene.

Experiments or calibrations are from Refs. 24–26. [Color figure can be viewed in the online issue, which is available at www.interscience.wiley.com.]

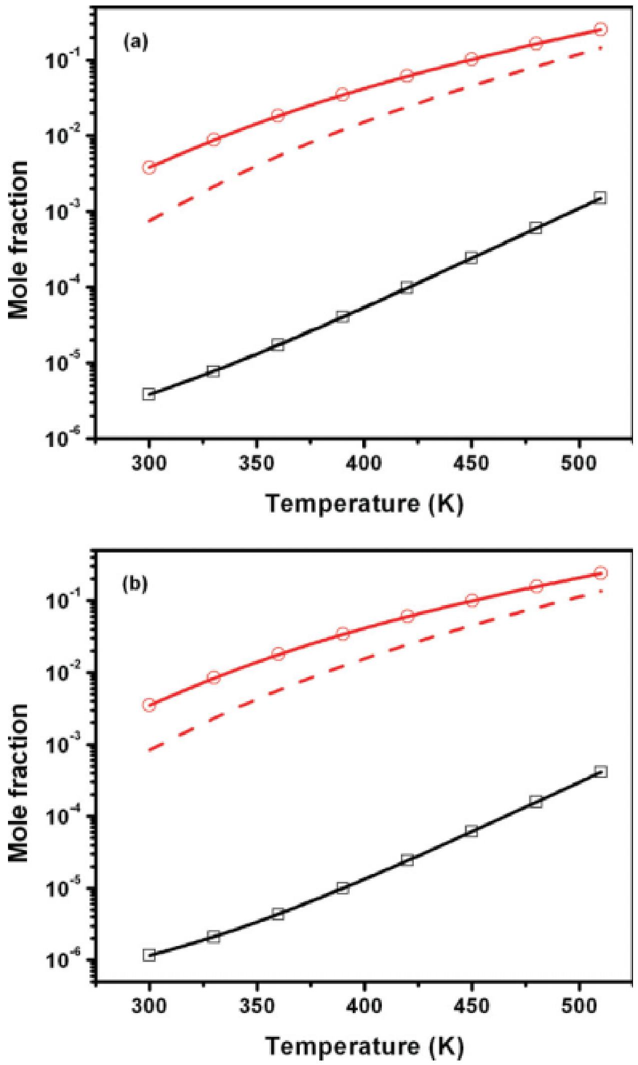

Figure 7. Same as Figure 5 but for (a) H_2O/1-methylnaphthalene, and (b) H_2O/1-ethylnaphthalene.

Experiments or calibrations are from Ref. 24. [Color figure can be viewed in the online issue, which is available at www.interscience.wiley.com.]

$$\chi_\alpha = \chi_\beta = \chi = \frac{1}{1 + 2\rho x_{\mathrm{w}}\chi\Delta^{\alpha\beta} + \sum_i 2\rho x_{\mathrm{ci}}\chi_i'\Delta^{\alpha\beta_i'}} \tag{2a}$$

$$\chi_{\alpha_i'} = \chi_{\beta_i'} = \chi_i' = \frac{1}{1 + 2\rho x_{\mathrm{w}}\chi\Delta^{\alpha\beta_i'}} \tag{2b}$$

where ρ is the molar density. As a consequence, Eq. 1 is further simplified to

$$\frac{F_{\mathrm{ass}}^{\mathrm{ex}}}{nRT} = 4x_{\mathrm{w}}\left(\ln\chi - \frac{\chi}{2} + \frac{1}{2}\right) + \sum_i 4x_{\mathrm{ci}}\left(\ln\chi_i' - \frac{\chi_i'}{2} + \frac{1}{2}\right). \tag{3}$$

Between molecules of water, the association strength is given by $\Delta^{\alpha\beta} = g\kappa^{\alpha\beta}$ [exp $(\varepsilon^{\alpha\beta}/k_{\mathrm{B}}T) - 1$]. Here, k_{B} is the Boltzmann constant, and $\kappa^{\alpha\beta}$ and $\varepsilon^{\alpha\beta}$ are the bonding volume and energy parameters of water, respectively. g is the contact value of the radial distribution function of hard-sphere mixture which can be approximated by that of the pure hard-sphere fluid as $g \approx \frac{1-0.5\eta}{(1-\eta)^3}$ with $\eta = \frac{b\rho}{4}$ and b the molecular volume parameter. Between molecules of water and pseudo-associating component i, the association strength is simply related to that between water molecules, i.e., $\Delta^{\alpha\beta_i'} = s_i\Delta^{\alpha\beta}$ where the temperature-dependent cross association factor s_i can be determined by fitting the experiments of binary mixtures together with the binary interaction coefficients k_{ij}.[10,11]

The methodology proposed above results in a unified model which drastically simplifies the computations. Other cross association schemes also can be used in modeling the pseudo-associating components. Two-site model is mathematically equivalent to the four-site model. However, one-site and three-site models will invalidate Eq. 2 and therefore complicate the computations. In the absence of water, the

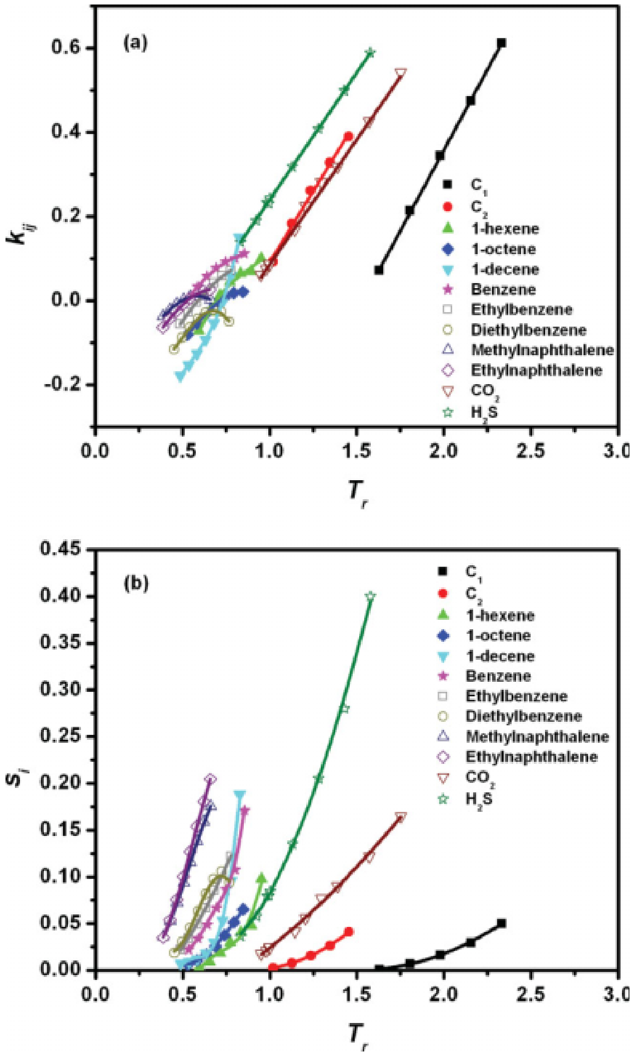

Figure 8. (a) Binary interaction coefficients and (b) cross association factors between water and non-water components as a function of reduced temperature of non-water species.

Lines are for guidance. [Color figure can be viewed in the online issue, which is available at www.interscience.wiley.com.]

Table 1. Mole Fractions of Water in C_1 Phase for H_2O/C_1 Mixture at High Pressures

	Mole Fraction of Water in C_1 Phase					
	758.4 bar			896.3 bar		
	Exp	Cal(ca)	Cal(nca)	Exp	Cal(ca)	Cal(nca)
313.9 K	4.72e-4	4.79e-4	4.22e-4	4.67e-4	4.57e-4	3.99e-4
366.5 K	3.13e-3	3.37e-3	2.29e-3	2.88e-3	3.21e-3	2.09e-3
422.04 K	0.0143	0.0159	0.0100	0.0137	0.0151	8.89e-3
466.5 K	0.040	0.0425	0.0273	–	–	–
477.5 K	0.051	0.0528	0.0344	–	–	–
	965.3 bar			1103.2 bar		
466.5 K	0.035	0.0391	0.0227	0.033	0.0376	0.0206
477.5 K	0.0494	0.0486	0.0285	0.0455	0.0466	0.0258

Experiments are from Ref. 27.
The columns with labels "ca" and "nca" represent the predictions with and without cross association, respectively.

resulting expression reduces to that of the original PR-EOS which has been successfully applied to the compositional reservoir simulators in the phase behavior calculations for hydrocarbon mixtures.

Results and Discussion

In Figures 1–4, we calculate the phase compositions for H_2O/C_1,[19,20] H_2O/C_2,[21,22] H_2O/CO_2,[23] and H_2O/H_2S[23] binary mixtures. For H_2O/C_1 mixture, the equilibrium is between the vapor and aqueous phases. For H_2O/C_2, H_2O/CO_2, and H_2O/H_2S mixtures, the jumps for the water composition in the nonaqueous phase at low temperatures are due to the change of the nonaqueous phase from vapor to liquid. It should be noted that for H_2O/C_2 mixture the sharp transition of the nonaqueous phase is hard to distinguish from the experiments. There is a slight decrease for H_2O/C_2 mixture but a substantial increase for H_2O/CO_2 and H_2O/H_2S mixtures of the water composition in the nonaqueous phase. The sudden transition corresponds to the appearance of the vapor-liquid-liquid three-phase point which disappears at high temperatures. To facilitate the comparison, the results without cross association are also presented.[7] The experiments are always perfectly reproduced and the accuracy is independent of the cross association in the aqueous phase. The accuracy of water mole fraction in the nonaqueous phase is greatly improved when cross association is taken into account. The calculated results with cross association are in excellent agreement with the experiments especially for H_2O/CO_2 and H_2O/H_2S mixtures in the liquid–liquid phase region. For H_2O/C_1 and H_2O/C_2 mixtures, the cross association is negligible when the pressure is not very high (e.g., lower than 200 bar), and, thus, the computations can be simplified.

Figures 5–7 present calculations and experiments for the mutual solubilities of H_2O/1-hexene, H_2O/1-octene, H_2O/1-decene, H_2O/benzene, H_2O/ethylbenzene, H_2O/*m*-diethylbenzene, H_2O/1-methylnaphthalene, and H_2O/1-ethylnaphthalene mixtures in liquid–liquid phase region.[24–26] For comparison, the results without cross association are also exhibited.[7] Similar to Figures 1–4, the hydrocarbon solubility in the aqueous phase is always perfectly reproduced. In the presence of cross association, the water solubility in the nonaqueous phase is drastically improved especially for the aromatic hydrocarbons.

The binary interaction coefficients and cross association factors are displayed in Figure 8 as a function of the reduced temperature of the nonwater species. For water/unsaturated-hydrocarbon mixtures, k_{ij} and s_i may not be very reliable because there is only one datapoint to determine them for

Table 2. Same as Table 1 But for Mole Fractions of Water in C_2 Phase for H_2O/C_2 Mixture at High Pressures

	Mole Fraction of Water in C_2 Phase					
	758.4 bar			896.3 bar		
	Exp	Cal(ca)	Cal(nca)	Exp	Cal(ca)	Cal(nca)
314.8 K	4.93e-4	6.42e-4	5.00e-4	4.49e-4	6.15e-4	4.73e-4
366.5 K	3.02e-3	3.89e-3	2.48e-3	2.87e-3	3.70e-3	2.29e-3
422.0 K	0.01498	0.0167	0.0105	0.01382	0.0157	9.50e-3
466.5 K	0.0455	0.0425	0.0286	–	–	–
	965.3 bar			1103.2 bar		
466.5 K	0.0401	0.0384	0.0243	0.0372	0.0364	0.0223

Experiments are from Ref. 27.

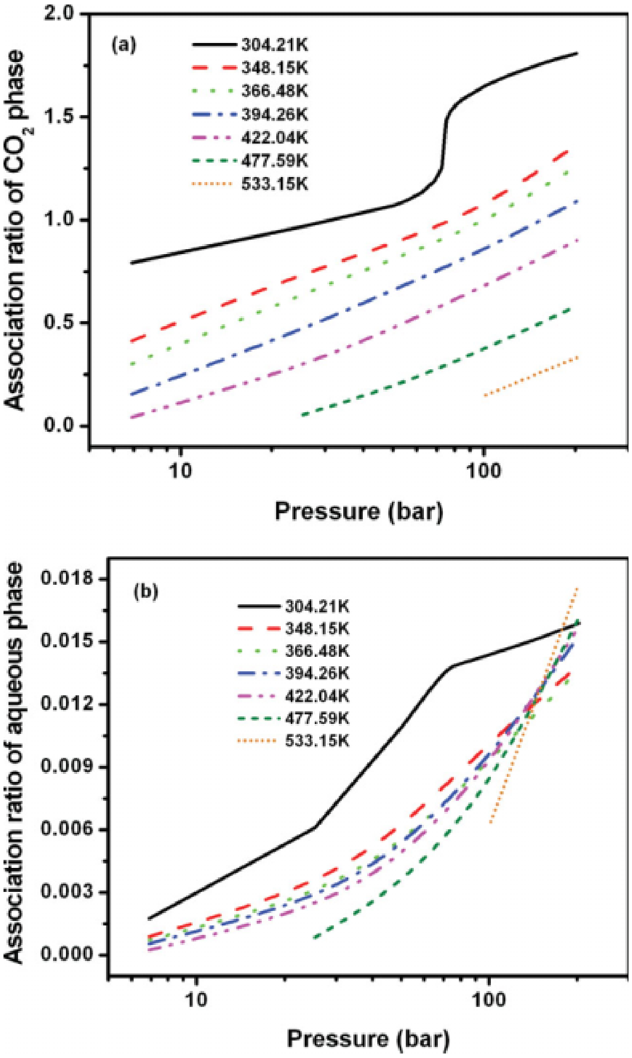

Figure 9. Association ratios of (a) CO_2 phase and (b) aqueous phase of H_2O/CO_2 mixture.

[Color figure can be viewed in the online issue, which is available at www.interscience.wiley.com.]

each temperature. As shown in Figure 8a, the binary interaction coefficients increase linearly with temperature for H_2O/C_1, H_2O/C_2, H_2O/CO_2, and H_2O/H_2S mixtures. It should be noted that in our recent work, due to the neglect of the cross association, the binary interaction coefficients only slightly change for H_2O/CO_2 mixture but decrease for H_2O/H_2S mixture with the increase of the temperature.[7] Different with those of the mixtures containing only nonwater species, the binary interaction coefficients of water-containing mixtures is strongly temperature-dependent. The "apparent" dispersion attraction between water and pseudo-associating species is influenced by the degree of self- and cross-association which is very sensitive to temperature. As presented in Figure 8b, the cross association factors demonstrate the systematic increasing trend with temperature when the nonwater species is C_1, C_2, CO_2, and H_2S; the exponential term of the association strength between water molecules drops more rapidly than that between water and pseudo-associating molecules when the temperature becomes higher. For other mixtures, k_{ij} and s_i also generally increases with temperature but the trend is not as systematic as that for H_2O/C_1, H_2O/C_2, H_2O/CO_2, and H_2O/H_2S mixtures. Our hypothesis is verified by examining these plots, i.e., the cross association related to aromatic hydrocarbons, CO_2 and particularly H_2S plays a dominant role in the determination of phase behavior. The cross association between water and saturated hydrocarbons is very weak and negligible except for H_2O/C_1 and H_2O/C_2 mixtures at very high pressures.[7]

For H_2O/C_1 and H_2O/C_2 mixtures, the cross association with water plays a significant role at high pressures. By using the binary interaction coefficients and cross association factors as given by Figure 8, we predict the mole fraction of water in the nonaqueous phase at very high pressures for these two mixtures in the two-phase region and compare them with the experiments from Ref. 27. The data from Ref. 27 were not used to determine the binary interaction coefficients and the cross association factors. Tables 1 and 2 present the predictions with and without the cross association at

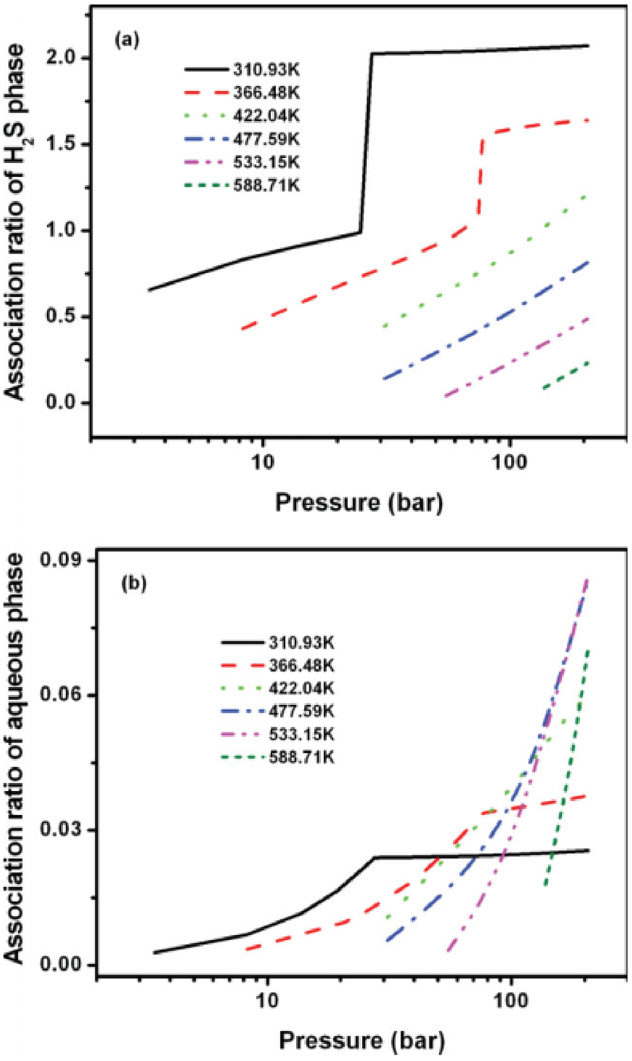

Figure 10. Same as Figure 9 but for H_2O/H_2S mixture.

[Color figure can be viewed in the online issue, which is available at www.interscience.wiley.com.]

Table 3. Vapor-Liquid Equilibrium of $H_2O/C_1/CO_2/H_2S$ Mixture

			Composition (Mole Fraction)					
			Aqueous			Vapor		
Temperature (K)	Pressure (bar)	Component	Exp	Cal(ca)	Cal(nca)	Exp	Cal(ca)	Cal(nca)
310.95	48.2	CH_4	2.76e-4	3.23e-4	3.18e-4	0.3040	0.3024	0.3025
		CO_2	9.3e-3	9.09e-3	9.43e-3	0.5945	0.5995	0.5994
		H_2S	5.03e-3	4.34e-3	4.07e-3	0.0998	0.0962	0.0966
		H_2O	0.9854	0.9863	0.9862	1.91e-3	1.85e-3	1.61e-3
	76.0	CH_4	4.66e-4	5.16e-4	5.06e-4	0.3031	0.3040	0.3041
		CO_2	0.0121	0.0124	0.0127	0.5970	0.5991	0.5989
		H_2S	5.40e-3	5.40e-3	5.03e-3	0.0982	0.0954	0.0959
		H_2O	0.9816	0.9817	0.9817	1.71e-3	1.48e-3	1.14e-3
	125.2	CH_4	7.96e-4	8.65e-4	8.48e-4	0.3029	0.3043	0.3045
		CO_2	0.0151	0.0147	0.0151	0.5967	0.5983	0.5983
		H_2S	5.95e-3	5.38e-3	5.01e-3	0.0985	0.0959	0.0964
		H_2O	0.9781	0.9791	0.9791	1.87e-3	1.60e-3	8.8e-4
	169.3	CH_4	9.9e-4	1.14e-3	1.11e-3	0.3021	0.3040	0.3044
		CO_2	0.0154	0.0153	0.0157	0.5963	0.5977	0.5980
		H_2S	6.08e-3	4.97e-3	4.63e-3	0.0996	0.0963	0.0968
		H_2O	0.9777	0.9786	0.9785	1.99e-3	2.00e-3	8.19e-4
380.35	83.6	CH_4	3.79e-4	3.96e-4	3.89e-4	0.2907	0.2956	0.2964
		CO_2	6.98e-3	7.79e-3	7.09e-3	0.5919	0.5877	0.5899
		H_2S	3.42e-3	3.26e-3	3.72e-3	0.0967	0.0953	0.0951
		H_2O	0.9894	0.9886	0.9888	0.0225	0.0214	0.0185
	129.3	CH_4	5.78e-4	6.12e-4	5.96e-4	0.2929	0.2980	0.2990
		CO_2	9.59e-3	0.0108	9.71e-3	0.5920	0.5899	0.5929
		H_2S	4.47e-3	4.17e-3	4.7e-3	0.0963	0.0952	0.0950
		H_2O	0.9854	0.9844	0.9850	0.0196	0.0169	0.0131
	171.7	CH_4	7.79e-4	8.02e-4	7.77e-4	0.2935	0.2990	0.3003
		CO_2	0.0113	0.0128	0.0115	0.5916	0.5903	0.5940
		H_2S	4.73e-3	4.65e-3	5.2e-3	0.0970	0.0952	0.0950
		H_2O	0.9834	0.9817	0.9825	0.0179	0.0155	0.0108
449.85	118.0	CH_4	7.17e-4	7.79e-4	7.65e-4	0.2641	0.2694	0.2723
		CO_2	7.95e-3	8.56e-3	8.42e-3	0.5575	0.5361	0.5419
		H_2S	3.74e-3	3.73e-3	3.93e-3	0.0848	0.0868	0.0875
		H_2O	0.9877	0.9868	0.9868	0.0950	0.1076	0.0982
	173.1	CH_4	1.1e-3	1.17e-3	1.14e-3	0.2762	0.2775	0.2813
		CO_2	0.0114	0.0119	0.0117	0.5520	0.5496	0.5571
		H_2S	4.78e-3	4.90e-3	5.13e-3	0.0870	0.0885	0.0894
		H_2O	0.9827	0.9820	0.9821	0.0848	0.0843	0.0722

The overall composition of each component on mole basis is 0.15 (C_1), 0.3 (CO_2), 0.05 (H_2S), and 0.5 (H_2O).
Experiments are from Ref. 28.
The columns with labels 'ca' and 'nca' represent the predictions with and without cross association, respectively.

very high pressures. For H_2O/C_1 mixture, the consideration of cross association drastically improves the performance of CPA. For H_2O/C_2 mixture at 314.8 and 366.5 K, the predictions without cross association are superior to those with cross association. It should be pointed out that the trend of experiments at 314.8 K from Ref. 27 is different with that at 310.93 K from Ref. 22. Such inconsistency problem does not exist between the two sets of data for H_2O/C_1 mixture from the two references.

In this work, we have observed that the good accuracy in the aqueous phase is readily achieved compared with that of the nonaqueous phase by adjusting the binary interaction coefficients. In the aqueous phase, the solubility of nonwater species is very low and the dominant process is the self association of water molecules, which has been accurately described. In the nonaqueous phase, the concentration of water is often low, and, therefore, the cross association between water and nonwater species may not be negligible. To illustrate our point, we quantify the importance of the cross association by defining the 'association ratio' as

$$\text{Association ratio (component } i) = \frac{(1-\chi_i'^{4})x_{\mathrm{ci}}}{(1-\chi^{4})x_{\mathrm{w}}}. \qquad (4)$$

In Eq. 4, the numerator is the number of moles of component i cross associated with water, and the denominator is the number of moles of associated water. A higher value of the association ratio implies more significant cross association. Figures 9 and 10 present the association ratios in the two phases for H_2O/CO_2 and H_2O/H_2S binary mixtures. The association ratio in the nonaqueous phase is always one or two orders of magnitude larger than that of the aqueous phase, which supports our assessment that cross association is the key element in the nonaqueous phase. Moreover, the cross association becomes more important with increased pressure or when the nonaqueous phase is liquid.

Table 4. Same as Table 3 But the Overall Composition is 0.05 (C_1), 0.05 (CO_2), 0.4 (H_2S), and 0.5 (H_2O)

			Composition (mole fraction)					
			Aqueous			Vapor/H_2S Liquid		
Temperature (K)	Pressure (bar)	Component	Exp	Cal(ca)	Cal(nca)	Exp	Cal(ca)	Cal(nca)
310.95	130.0	CH_4	8.59e-4	9.75e-4	8.88e-4	0.0891	0.1013	0.1021
		CO_2	3.62e-3	2.74e-3	2.68e-3	0.0994	0.0991	0.0998
		H_2S	0.0291	0.0303	0.0271	0.8016	0.7882	0.7972
		H_2O	0.9666	0.9659	0.9693	9.32e-3	0.0114	8.49e-4
	164.6	CH_4	8.82e-4	1.04e-3	9.46e-4	0.0891	0.1013	0.1022
		CO_2	3.81e-3	2.83e-3	2.76e-3	0.1061	0.0993	0.1001
		H_2S	0.0281	0.0306	0.0273	0.7958	0.7873	0.7968
		H_2O	0.9672	0.9655	0.9690	9.05e-3	0.0121	8.31e-4
380.35	75.6	CH_4	1.55e-4	1.60e-4	1.56e-4	0.1182	0.0980	0.0988
		CO_2	1.25e-3	1.43e-3	1.27e-3	0.1112	0.0966	0.0975
		H_2S	0.0304	0.0289	0.0315	0.7485	0.7809	0.7843
		H_2O	0.9682	0.9695	0.9670	0.0253	0.0244	0.0194
	122.7	CH_4	3.32e-4	3.44e-4	3.21e-4	0.1060	0.1008	0.1022
		CO_2	2.26e-3	2.26e-3	1.96e-3	0.1148	0.0984	0.1000
		H_2S	0.0361	0.0372	0.0399	0.7528	0.7778	0.7850
		H_2O	0.9613	0.9600	0.9577	0.0264	0.0229	0.0127
	169.2	CH_4	6.06e-4	5.78e-4	5.18e-4	0.1207	0.1002	0.1029
		CO_2	3.34e-3	2.81e-3	2.43e-3	0.1176	0.0978	0.1006
		H_2S	0.0392	0.0384	0.0417	0.7322	0.7709	0.7861
		H_2O	0.9568	0.9582	0.9554	0.0295	0.0311	0.0104
449.85	110.0	CH_4	3.50e-4	3.36e-4	3.12e-4	0.1092	0.0905	0.0924
		CO_2	1.64e-3	1.69e-3	1.56e-3	0.1078	0.0892	0.0912
		H_2S	0.0286	0.0341	0.0334	0.6896	0.6979	0.7126
		H_2O	0.9694	0.9638	0.9647	0.0938	0.1224	0.1037
	181.7	CH_4	7.15e-4	7.16e-4	6.12e-4	0.0928	0.0933	0.0967
		CO_2	2.92e-3	2.95e-3	2.55e-3	0.0914	0.0909	0.0944
		H_2S	0.0517	0.0520	0.0484	0.704	0.7112	0.7379
		H_2O	0.9454	0.9433	0.9485	0.113	0.1035	0.0710

At 310.95K, the equilibrium is between the aqueous phase and H_2S liquid phase.

On the basis of binary interaction coefficients and cross association factors presented above without any adjustments, we perform the predictions for phase composition of H_2O/C_1/CO_2/H_2S quaternary mixture in two- and three-phase regions. Results are displayed in Tables 3–5.[28] Here, the cross association between water and C_1 is not accounted for because the pressure is lower than 200 bar. The binary interaction coefficients of H_2O–C_1, C_1–CO_2, C_1–H_2S and CO_2–H_2S can be found in.[7,29,30] For the comparison purpose, the results without cross association are also presented.[7] Similar to binary mixtures, the prediction of water mole fraction in the vapor phase and particularly in the H_2S liquid phase is significantly improved with cross association. The accuracy is nearly unaffected for other components. The effect of cross association to this quaternary mixture is highlighted by the average absolute deviations (AAD) shown in Table 6.

Accurate description of the density of water saturated with CO_2 is very important in modeling of CO_2 sequestration and migration in saline aquifers, oceans, and depleted oil and gas reservoirs and in the simulation of CO_2-related enhanced oil recovery. Different with other gases, dissolution of CO_2 in water often causes the increase of the density. Because such density increase is generally not large, the accurate estimation of the pure water density is the necessity. In this work, we use a polynomial to describe temperature-dependent volume translation for pure water which is determined from the best fit of the difference of the saturated liquid molar volume between the experiments and calculations up to 600 K, i.e.,

Table 5. Same as Table 4 But for Vapor-Liquid-Liquid Equilibrium

			Composition (Mole Fraction)								
			H_2S Liquid			Aqueous			Vapor		
Temperature (K)	Pressure (bar)	Component	Exp	Cal(ca)	Cal(nca)	Exp	Cal(ca)	Cal(nca)	Exp	Cal(ca)	Cal(nca)
310.95	62.6	CH_4	0.0653	0.0616	0.0642	4.9e-4	5.98e-4	5.53e-4	0.3213	0.3596	0.3527
		CO_2	0.1049	0.0971	0.0981	3.5e-3	2.61e-3	2.54e-3	0.1739	0.1219	0.1213
		H_2S	0.8197	0.8292	0.8369	0.0284	0.0310	0.0276	0.5028	0.5169	0.5248
		H_2O	0.0101	0.0122	8.85e-4	0.9677	0.9659	0.9694	2.14e-3	1.63e-3	1.26e-3
338.75	84.3	CH_4	0.0580	0.0641	0.0674	3.85e-4	4.15e-4	3.8e-4	0.1872	0.2057	0.1919
		CO_2	0.0904	0.0922	0.0941	2.72e-3	2.47e-3	2.17e-3	0.1484	0.1185	0.1176
		H_2S	0.8287	0.8264	0.8358	0.0321	0.0326	0.0346	0.6557	0.6704	0.6870
		H_2O	0.0212	0.0174	2.72e-3	0.9684	0.9645	0.9628	8.66e-3	5.44e-3	3.52e-3

$$c_w = a_0 + a_1 T_{rw} + a_2 T_{rw}^2 + a_3 T_{rw}^3 + a_4 T_{rw}^4 + a_5 T_{rw}^5 + a_6 T_{rw}^6$$

where c_w is the volume translation parameter in the unit of "L/mol" and T_{rw} is the reduced temperature. The coefficients are $a_0 = 0.1214789046$, $a_1 = -1.1152038536$, $a_2 = 4.3159229705$, $a_3 = -8.9395416719$, $a_4 = 10.3968272712$, $a_5 = -6.4222352433$, and $a_6 = 1.6442114295$. The AAD between the experiments and calculations is about 0.02% for the molar volume of pure water. The "true" molar volume of the mixture is calculated from $v^{\mathrm{True}} = v^{\mathrm{EOS}} + (x_w c_w + x_{CO_2} c_{CO_2})$ where v^{EOS} is the "apparent" molar volume obtained from the EOS. The volume translation parameter for CO_2 is assumed to be a constant and determined from fitting the experiments of CO_2-saturated water densities ($c_{CO_2} = -0.00314457$ L/mol).[31] It should be noted that the value is different with that of pure CO_2 from the PR-EOS. CO_2 is a "special" substance compared with hydrocarbons because its saturated liquid densities cannot be matched by simply applying a constant volume translation to the results from the PR-EOS.

As displayed in Figure 11, a fairly good agreement is achieved between the experiments and calculations for the CO_2-saturated water density in the examined temperature range by considering the volume translations for both water and CO_2. The density of the CO_2-saturated water strongly depends on the state of the coexisting CO_2 phase. The sharp slope transitions at the low temperatures denote the CO_2 phase changes from vapor to liquid. For comparison, the densities of pure water are also calculated and plotted in the same figure. Under the examined temperatures and pressures, pure water is in the single-liquid phase. For all the cases, the density of the CO_2-saturated water is always higher than that of pure water. The largest increase which is about 2% appears at the highest pressure of the lowest temperature and the difference becomes smaller as the pressure decreases or the temperature increases.

Conclusions

The accuracy of CPA approach we proposed recently for the water-containing mixtures has been significantly improved by applying the "pseudo-association" concept. The unsaturated hydrocarbons, methane, ethane, CO_2 and H_2S are treated as pseudo-associating components, i.e., they only associate with water but do not associate with themselves. This cross association with water can be accurately described by using the same theoretical framework as the association of water molecules.

The cross association is likely due to polar–polar interactions between water and CO_2 or H_2S or due to polar-induced polar interactions between water and hydrocarbons, which has not been properly described by our previous CPA approach. For H_2O/C_1 and H_2O/C_2 mixtures, although C_1 and C_2 are saturated and nonpolar, the strong permanent polar moments of water molecules can cause the temporary separation of the centers of positive and negative charges of C_1 and C_2 molecules.

Table 6. Average Absolute Deviations of each Component for $H_2O/C_1/CO_2/H_2S$ Mixture With and Without Cross Association

	AAD (%)	
Component	With cross Association (ca)	Without Cross Association (nca)
CH_4	7.59	6.70
CO_2	8.21	8.28
H_2S	4.11	5.91
H_2O	7.82	24.24

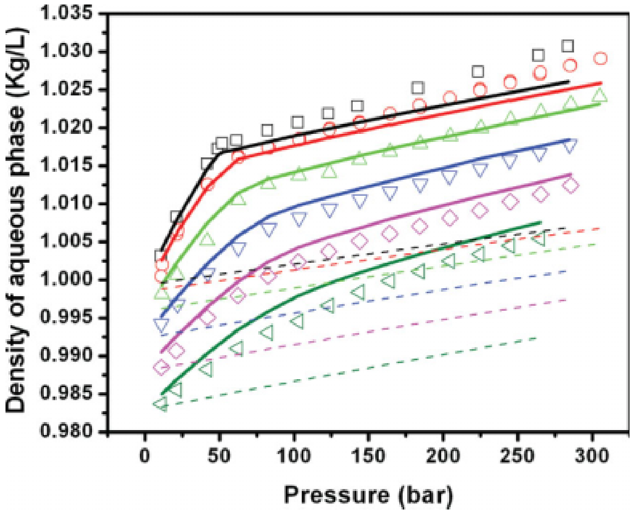

Figure 11. Density of CO_2-saturated water (symbols: experiments from Ref. 31; solid lines: calculations) and of pure water (dash lines: calculations).

For each set, from top to bottom, the temperatures are 288, 293, 303, 313, 323 and 333 K. [Color figure can be viewed in the online issue, which is available at www.interscience.wiley.com.]

The modified approach enhances the accuracy in phase behavior calculations for H_2O/C_1, H_2O/C_2, H_2O/CO_2, H_2O/H_2S, H_2O/1-hexene, H_2O/1-octene, H_2O/1-decene, H_2O/benzene, H_2O/ethylbenzene, H_2O/*m*-diethylbenzene, H_2O/1-methylnaphthalene, H_2O/1-ethylnaphthalene, and $H_2O/C_1/CO_2/H_2S$ mixtures. We also reliably reproduce the density increase when water is saturated with CO_2 by introducing the temperature-dependent and constant volume translations for water and for CO_2, respectively.

Acknowledgements

The authors are grateful to the financial support from the industrial sponsors of RERI.

Literature Cited

1. Kontogeorgis GM, Voutsas EC, Yakoumis IV, Tassios DP. An equation of state for associating fluids. *Ind Eng Chem Res.* 1996;35:4310–4318.
2. Wu JZ, Prausnitz JM. Phase equilibria for systems containing hydrocarbons, water, and salt: an extended Peng-Robinson equation of state. *Ind Eng Chem Res.* 1998;37:1634–1643.
3. Yakoumis IV, Kontogeorgis GM, Voutsas EC, Hendriks EM, Tassios DP. Prediction of phase equilibria in binary aqueous systems containing alkanes, cycloalkanes, and alkenes with the cubic-plus-association equation of state. *Ind Eng Chem Res.* 1998;37:4175–4182.
4. Oliveira MB, Coutinho JAP, Queimada AJ. Mutual solubilities of hydrocarbons and water with the CPA EoS. *Fluid Phase Equilibria.* 2007;258:58–66.

5. Voutsas EC, Boulougouris GC, Economou IG, Tassios DP. Water/hydrocarbon phase equilibria using the thermodynamic perturbation theory. *Ind Eng Chem Res*. 2000;39:797–804.
6. Kontogeorgis GM, Michelsen ML, Folas GK, Derawi S, von Solms N, Stenby EH. Ten years with the CPA (cubic-plus-association) equation of state. I. Pure compounds and self-associating systems. *Ind Eng Chem Res*. 2006;45:4855–4868.
7. Li ZD, Firoozabadi A. Cubic-plus-association (CPA) equation of state for water-containing binary, ternary, and quaternary mixtures in two and three phases. Supporting Materials.
8. Folas GK, Kontogeorgis GM, Michelsen ML, Stenby EH. Application of the cubic-plus-association equation of state to mixtures with polar chemicals and high pressures. *Ind Eng Chem Res*. 2006;45: 1516–1526.
9. von Solms N, Michelsen ML, Kontogeorgis GM. Applying association theories to polar fluids. *Ind Eng Chem Res*. 2004;43:1803–1806.
10. Perakis C, Voutsas E, Magoulas K, Tassios D. Thermodynamic modeling of the vapor-liquid equilibrium of the water/ethanol/CO2 system. *Fluid Phase Equilibria*. 2006;243:142–150.
11. Perakis CA, Voutsas EC, Magoulas KG, Tassios DP. Thermodynamic modeling of the water plus acetic acid + CO2 system: the importance of the number of association sites of water and of the nonassociation contribution for the CPA and SAFT-type models. *Ind Eng Chem Res*. 2007;46:932–938.
12. Voutsas E, Perakis C, Pappa G, Tassios D. An evaluation of the performance of the cubic-plus-association equation of state in mixtures of non-polar, polar and associating compounds: towards a single model for non-polymeric systems. *Fluid Phase Equilibria*. 2007; 261:343–350.
13. Wertheim MS. Fluids with highly directional attractive forces. I. Statistical thermodynamics. *J Stat Phys*. 1984;35:19–34.
14. Wertheim MS. Fluids with highly directional attractive forces. II. Thermodynamic perturbation-theory and integral-equations. *J Stat Phys*. 1984;35:35–47.
15. Wertheim MS. Fluids of dimerizing hard-spheres, and fluid mixtures of hard-spheres and dispheres. *J Chem Phys*. 1986;85:2929–2936.
16. Wertheim MS. Fluids with highly directional attractive forces. III. Multiple attraction sites. *J Stat Phys*. 1986;42:459–476.
17. Wertheim MS. Fluids with highly directional attractive forces. IV. Equilibrium polymerization. *J Stat Phys*. 1986;42:477–492.
18. Wertheim MS. Thermodynamic perturbation-theory of polymerization. *J Chem Phys*. 1987;87:7323–7331.
19. Culberson OL, McKetta JJ. Phase equilibria in hydrocarbon-water systems. III. The solubility of methane in water at pressures to 10,000 psia. *Trans Am Inst Min Metall Eng*. 1951;192:223–226.
20. Olds RH, Sage BH, Lacey WN. Phase equilibria in hydrocarbon systems—composition of the dew-point gas of the methane-water system. *Ind Eng Chem*. 1942;34:1223–1227.
21. Culberson OL, McKetta JJ. Phase equilibria in hydrocarbon-water systems. II. The solubility of ethane in water at pressures to 10,000 Psi. *Trans Am Inst Min Metall Eng*. 1950;189:319–322.
22. Reamer HH, Olds RH, Sage BH, Lacey WN. Composition of dew-point gas in ethane-water system. *Ind Eng Chem*. 1943;35:790–793.
23. Gillespie PC, Wilson GM. *Vapor-Liquid and Liquid-Liquid Equilibria: Water-Methane, Water-Carbon dioxide, Water-Hydrogen Sulfide, Water-nPentane, and Water-Methane-nPentane*. Provo, Utah: GPA Research Report RR-48, Wiltec Research Co. Inc., 1982.
24. Economou IG, Heidman JL, Tsonopoulos C, Wilson GM. Mutual solubilities of hydrocarbons and water. III. 1-Hexene, 1-octene, C-10-C-12 hydrocarbons. *AIChE J*. 1997;43:535–546.
25. Heidman JL, Tsonopoulos C, Brady CJ, Wilson GM. High-temperature mutual solubilities of hydrocarbons and water. II. Ethylbenzene, ethylcyclohexane, and normal-octane. *AIChE J*. 1985;31: 376–384.
26. Tsonopoulos C, Wilson GM. High-temperature mutual solubilities of hydrocarbons and water. I. Benzene, cyclohexane and normal-hexane. *AIChE J*. 1983;29:990–999.
27. Yarrison M, Cox KR, Chapman WG. Measurement and modeling of the solubility of water in supercritical methane and ethane from 310 to 477 K and pressures from 3.4 to 110 MPa. *Ind Eng Chem Res*. 2006;45:6770–6777.
28. Huang SSS, Leu AD, Ng HJ, Robinson DB. The phase-behavior of 2 mixtures of methane, carbon-dioxide, hydrogen-sulfide, water. *Fluid Phase Equilibria*. 1985;19:21–32.
29. Firoozabadi A. *Thermodynamics of Hydrocarbon Reservoirs*. New York: McGraw-Hill, 1999.
30. Arbabi S, Firoozabadi A. Near-critical phase behavior of reservoir fluids using equations of state. *SPE Adv Technol*. 1995;139–145.
31. Hebach A, Oberhof A, Dahmen N. Density of water plus carbon dioxide at elevated pressures: measurements and correlation. *J Chem Eng Data*. 2004;49:950–953.

Manuscript received May 31, 2008, and revision received Oct. 1, 2008.